Pergamon

Tetrahedron 56 (2000) 6969–6977

TETRAHEDRON

Generation and Direct Observation of the 9-Fluorenyl Cation in Non-acidic Zeolites

Melanie A. O'Neill, Frances L. Cozens* and Norman P. Schepp

Department of Chemistry, Dalhousie University, Halifax, Nova Scotia, Canada, B3H 4J3

Received 20 February 2000; revised 13 March 2000; accepted 15 March 2000

Abstract—9-Alkyl-9-fluorenyl cations and the parent 9-fluorenyl cation are generated via photoheterolysis of the corresponding 9-fluorenols within alkali metal zeolites such as LiY, NaY and Naβ, and observed directly using nanosecond laser flash photolysis. The observation of the highly reactive and highly unstable 9-fluorenyl cation under these conditions provides a remarkable example of the extraordinary ability of non-proton exchanged zeolites to provide kinetic stabilisation for electrophilic guests. The reactivity of the carbocations is found to be highly influenced by the nature of the alkali metal counterion as well as the inclusion of cosolvents within the zeolite matrix. The availability of several reaction pathways, other than heterolysis, to photoexcited 9-fluorenols within the zeolite cavities is also demonstrated and shown to be modified by co-adsorbed protic reagents in a manner consistent with solvent-assisted dehydroxylation.

Introduction

Zeolites are aluminosilicate host materials and catalysts constructed of $[SiO_4]^{4-}$ and $[AlO_4]^{5-}$ tetrahedra linked via oxygen bridges creating an open framework structure of molecular-sized pores, channels and cavities. Over the past several years, there has been considerable interest in the chemistry of carbocations generated within the cavities of the proton exchanged, acidic forms of these materials, especially with respect to direct spectroscopic detection and characterisation.[1–15] Results from numerous studies in this area have led to tremendous advances in our understanding of the nature of stable carbocations within acidic zeolites and the reactivity of carbocation intermediates in zeolite catalysis. In particular, such research has contributed to the emerging picture of Brønsted zeolites not as superacid solid materials as once envisioned, but as strong acids whose ability to stabilise electrophilic species and influence their reactivity is largely tied to the dynamic role of the zeolite framework in carbocation chemistry.[12] Thus, although several types of relatively stabilised carbocations such as triarylmethyl,[4,9] xanthylium,[3,5,16] dibenzotropylium,[16] indanyl[10] and cyclopentenyl[11] cations can be detected as stable ions in acidic zeolites, other more reactive carbocations such as phenethyl[6,10] cations do not persist as stable ions within these environments. The reactivity of such species is consistent with current predictions regarding the stability of reactive carbocations within these acidic environments.[12,14] However, these studies do not preclude these carbocations as *transient* intermediates within acidic zeolite catalysis, but do suggest that the catalytic role of zeolite properties other than acidity warrants further investigation.

In recent years, we have been studying the chemistry of carbocations generated within non-proton exchanged zeolites. Examining the behaviour of carbocations under these conditions provides information not available from studies using acid zeolites in which the high acidity of the environment dominates over other possible roles that the solid-state material might play. To date, we have generated as transient species several different kinds of carbocations such as the xanthylium cation,[17] cumyl cations,[18,19] and 1,1-diarylmethyl cations.[20] While each of these are reactive carbocations, they all possess a significant degree of stabilisation that allows them to be sufficiently long-lived to observe using nanosecond diffuse reflectance techniques. These studies have led us to examine carbocations that are less thermodynamically stable to determine if the properties of non-acid zeolites are suitable to support the formation and enhance the lifetime of these kinds of highly reactive electrophilic intermediates. The highly reactive carbocations we chose to examine in the present work are 9-alkyl-9-fluorenyl cations and especially the parent 9-fluorenyl cation. These carbocations possess unusually high reactivity and low thermodynamic stability in solution.[21–23] In addition, they are readily generated in solution from 9-fluorenols via a photoheterolysis mechanism that is sensitive to the presence and ionising ability of the protic media.[24–26] This system therefore also provides an opportunity to examine the effect of zeolite structure on a

Keywords: zeolites; cation-exchange; 9-fluorenyl cation; reactivity; laser photolysis.

* Corresponding author. E-mail: fcozens@is.dal.ca

0040–4020/00/$ - see front matter
PII: S0040-4020(00)00518-4

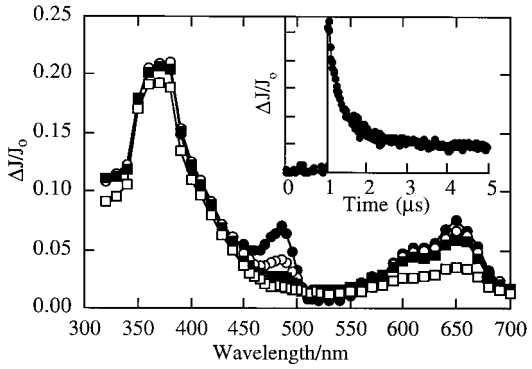

Figure 1. Transient diffuse reflectance spectrum generated upon 308 nm excitation of 9-methyl-9-fluorenol in NaY under an atmosphere of oxygen. Spectra were taken (●) 140 ns, (○) 360 ns, (■) 760 ns, (□) 7.0 μs after the laser pulse. Insert shows the decay of the transient at 485 nm in oxygen saturated NaY.

photochemical reaction characterised by photoheterolysis and significant charge separation in the rate determining step.

Results

Laser photolysis of 9-alkyl-9-fluorenol in alkali metal zeolites

Laser irradiation of 9-methyl-9-fluorenol in oxygen-saturated, dry NaY (Si/Al=2.4) gives a transient diffuse reflectance spectrum with a number of distinct absorption bands, Fig. 1. One of these absorption bands is centred at 485 nm. The transient responsible for this band is not stable, and decays completely within approximately 2 μs after the laser pulse. The decay fits well to a first-order expression to give a rate constant of $3.5\times10^6\ s^{-1}$, Table 1. The rate constant for the disappearance of the 485 nm band increases strongly in the presence of added nucleophiles like water in a manner consistent with the behaviour of a carbocation species. There is also a close similarity between the maximum of the transient at 485 nm and that for the 9-methyl-9-fluorenyl cation generated previously in solution.[22,23] On the basis of these observations, we can confidently assign the transient species at 485 nm as the 9-methyl-9-fluorenyl cation generated by photoheterolysis from 9-methyl-9-fluorenol in NaY (Scheme 1, path a).

Removal of oxygen caused a slight increase in the intensity of the absorption at 485 nm and revealed an additional slow decay that followed the fast decay of the carbocation. Since carbocations are not influenced by the presence of oxygen, this small oxygen effect is due to the presence of a second transient species that also has strong absorption near 485 nm. A reasonable assignment for this second transient is the 9-methyl-9-fluorenyl radical. This radical has a maximum absorption at 485 nm, is expected to be quenched by oxygen, and has been observed previously as a product from the photohomolysis (Scheme 1, path b) of 9-fluorenol derivatives.[28]

Table 1. First order decay rate constants for 9-R-9-fluorenyl cations and other carbocations in the alkali metal zeolites LiY, NaY and Naβ

R	$k_{decay}/10^6\ s^{-1}$		
	LiY	NaY	Naβ
H	2.95±0.10	6.59±0.20	Not observed
Me	1.85±0.13	3.45±0.06	0.87±0.016
Et	1.38±0.04	3.63±0.12	0.83±0.04
*i*Pr	1.44±0.02	5.62±0.08	0.81±0.05
Ph_2CH^+	0.55±0.08[a]	0.60±0.06[a]	
4-$CH_3OPhC(CH_3)_2^+$	0.04±0.01[b]	0.22±0.02[b]	

[a] Ref. 20.
[b] Refs. 18,19.

The most intense band produced upon laser irradiation of 9-methyl-9-fluorenol in NaY is centred at 370 nm, Fig. 1. Unlike the carbocation at 485 nm, which decays rapidly over a few microseconds, the species responsible for the absorption band at 370 nm shows no decay, even over a time as long as several milliseconds, which is the longest time-scale accessible on our laser system. In fact, this species is sufficiently long-lived to be detected by conventional diffuse reflectance spectroscopy. Over the long time-scales available with the conventional instrument, the species at 370 nm was observed to decay over several minutes with a rate constant of $0.0144\ s^{-1}$. A long-lived transient with a similar absorption maximum has been previously detected upon laser photolysis of 9-fluorenol in methanol,[21] and was assigned as a metastable triene isomer generated by photoinduced rearrangement, Scheme 1, path (c). While this assignment was not established rigorously, there is literature precedent for similar rearrangements of related compounds,[29] and it has recently been shown that 3,5-dimethoxybenzyl acetate undergoes a comparable photoinduced rearrangement in methanol.[30] Based on these considerations, we assign this transient to the triene isomer produced by a photoinduced intramolecular rearrangement of the alcohol moiety, Scheme 1, path (c).

A long wavelength absorption band near 640 nm is also evident in the transient diffuse reflectance spectra shown in Fig. 1. This 640 nm band is very characteristic of the radical cation of 9-methyl-9-fluorenol in solution.[22,23,27] The absorption band at 640 nm is therefore attributed to the 9-methyl-9-fluorenol radical cation produced by photoionization, Scheme 1, path (d). The spectrum of the 9-methyl-9-fluorenol radical cation in solution also shows the presence of a second absorption band of similar intensity at 370 nm.[22,23,27] In our diffuse reflectance spectra, this band is somewhat obscured by strong luminescence at short-time scales in this region, but can nonetheless be observed as a fairly fast decay superimposed above the static absorption of the triene isomer at the same wavelength. The rate constant for the fast decay at 370 nm is the same as the decay at 640 nm ($k=6\times10^5\ s^{-1}$), indicating that both bands due to the radical cation are observed in the zeolite. In addition, the transient absorbing at 370 and 640 nm is not affected by the presence of oxygen, which is consistent with the known behaviour of fluorene radical cations.

In summary at least four distinct reaction pathways are available to 9-methyl-9-fluorenol upon photochemical excitation within the cavities of dry NaY, Scheme 1. Photoheterolysis, path (a), takes place to generate the reactive 9-methyl-9-fluorenyl cation characterised by an absorption

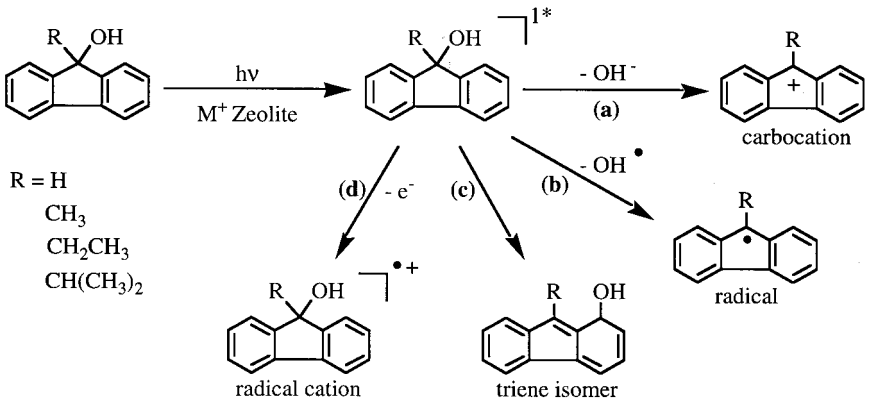

Scheme 1.

maxima at 485 nm, and a rapid decay with a rate constant of 3.5×10^6 s^{-1}. Photohomolysis, path (b), produces the corresponding radical that is completely quenched by the introduction of oxygen within the zeolite. Photoinduced rearrangement, path (c), leads to the metastable triene isomer which has an intense absorption maxima at 370 nm and shows no decay over times as long as 1 ms. Photoionization, path (d), generates the radical cation with absorption at 370 and 640 nm. This transient is significantly longer-lived than the reactive carbocation, decays with a rate constant of 6×10^5 s^{-1} in NaY and is unaffected by the addition of oxygen to the sample.

In LiY, laser photolysis of 9-methyl-9-fluorenol under dry conditions gives results analogous to those in NaY. Under vacuum conditions, bands due to the presence of both the 9-methyl-9-fluorenyl cation and radical at 485 nm are observed, with the radical being completely quenched upon subsequent addition of oxygen to the sample. A long-lived band at 370 nm due to the metastable triene isomer is also observed, and again this band is sufficiently long-lived to be detected by conventional diffuse reflectance. Finally, the radical cation of 9-methyl-9-fluorenol is clearly detected with absorption bands at both 370 and 640 nm.

An important difference between the results in LiY and those in NaY is the lifetime of the 9-methyl-9-fluorenyl cation. In LiY, the carbocation decays in a first-order manner with rate constant of 1.9×10^6 s^{-1}. This rate constant is significantly slower by a factor of 1.85 than the rate constant of 3.5×10^6 s^{-1} in NaY. In other alkali metal Y-zeolites, KY, RbY and CsY, the 9-methyl-9-fluorenyl cation could not be detected at all; only the metastable triene isomer, the 9-methyl-9-fluorenol radical cation and the 9-methyl-9-fluorenyl radical were observed. Our inability to observe the reactive carbocation in these zeolites may indicate that the photoheterolysis reaction does not take place under these conditions. However, another possibility is that the carbocation is still photogenerated, but has a lifetime in the larger alkali metal exchanged zeolites that is too short to be measured with our nanosecond laser system. This is in agreement with the observation that the reactivity of the 9-methyl-9-fluorenyl cation increases significantly as the size of the cation is increased from LiY to NaY, and also with other results we have obtained showing that the lifetimes of carbocations in alkali metal exchanged zeolites decrease considerably as the size of the alkali metal counterion increases.[18] The increase in the reactivity of the carbocation is presumably due to increased nucleophilicity of active site oxygens caused by the weaker interactions between large alkali metal cations and the zeolite framework. The nucleophilic attack of the active oxygen sites of the framework to the electrophilic carbocation centre generates framework bound alkoxy species.

The 9-methyl-9-fluorenyl cation can also be generated and directly observed in the highly dealuminated Naβ (Si/Al=18). Along with the triene isomer at 370 nm and the 9-methyl-9-fluorenol radical cation at 640 nm, the characteristic absorption band of the 9-methyl-9-fluorenyl cation at 485 nm is distinctly observed following laser photolysis of 9-methyl-9-fluorenol in oxygen saturated Naβ. In this zeolite, the carbocation decays in a first-order manner with a rate constant of 0.87×10^6 s^{-1} that is four-fold smaller than that in NaY, Table 1.

Similar results to those described above for the 9-methyl-9-fluorenyl cation were obtained with the 9-ethyl- and 9-*iso*-propyl-9-fluorenyl cations generated within LiY, NaY and Naβ from the appropriate fluorenol derivatives. In each case, the carbocations were generated and then decayed with rate constants similar to those for the methyl derivative, Table 1. In addition, carbocation formation was accompanied by the presence of the triene isomer at 370 nm and the radical cation at 370 and 640 nm. Under vacuum conditions, the 9-alkyl-9-fluorenyl radicals were also observed.

Laser photolysis of 9-fluorenol in alkali metal zeolites

The results described above clearly indicate that LiY and NaY are sufficiently non-nucleophilic to support the formation of reactive 9-alkyl-9-fluorenyl cations. However, while these carbocations are reactive, they are still stabilised by the alkyl group at the 9-position, and may not fully reflect the ability of alkali metal zeolites to support the presence of very reactive carbocations. As a result, we carried out a series of experiments with 9-fluorenol, which upon photoheterolysis would produce the parent, unstabilised 9-fluorenyl cation.

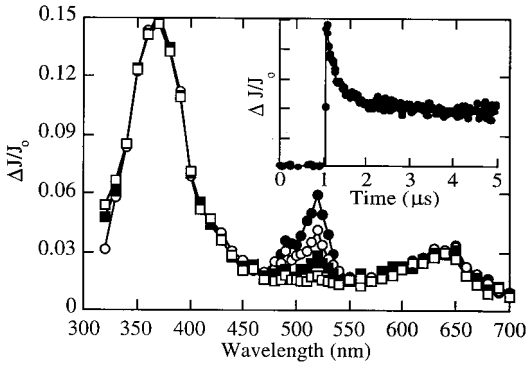

Figure 2. Transient diffuse reflectance spectrum generated upon 308 nm excitation of 9-fluorenol in LiY under an atmosphere of oxygen. Spectra were taken (●) 120 ns, (○) 480 ns, (■) 1.18 μs, (□) 3.12 μs after the laser pulse. Insert shows the decay of the transient at 515 nm in oxygen saturated LiY.

Laser irradiation of 9-fluorenol in oxygen-saturated, dry LiY (Si/Al=2.4) gives a transient diffuse reflectance spectrum, Fig. 2, with features that are very similar to those observed upon laser irradiation of 9-methyl-9-fluorenol in the same zeolite. A large band at 370 nm that does not decay on the time-scale of the laser system is clearly observed. We assign this transient as the metastable triene isomer on the basis of the same reasoning described above for the triene isomer generated from 9-methyl-9-fluorenol. A weak, long wavelength absorption band near 640 nm is also evident in the transient diffuse reflectance spectrum shown in Fig. 2. This 640 nm band is attributed to the 9-fluorenol radical cation[22,23,27] produced by photoionization of 9-fluorenol within LiY.

More interesting than the formation of the transients described above is the presence of an absorption band at 515 nm with a shoulder at 485 nm. This absorption is virtually identical to the absorption band of the 9-fluorenyl cation in solution as established by picosecond laser photolysis in aqueous methanol[23] and nanosecond laser photolysis in 1,1,1,3,3,3-hexafluoro-2-propanol (HFIP).[22] The characteristic absorption maxima and band shape strongly suggest that the transient species at 515 nm in LiY is due to the 9-fluorenyl cation. The reactivity of the transient in LiY is also consistent with this assignment. The transient is very short-lived in LiY, decaying with a first-order rate constant of 2.9×10^6 s^{-1}. In addition, the transient species absorbing at 515 nm is unreactive towards oxygen, but reacts rapidly with co-adsorbed nucleophiles such as water, as typically observed for carbocation species. We thus identify the transient at 515 nm as the 9-fluorenyl cation generated by photoheterolysis of 9-fluorenol within the cavities of LiY.

Laser irradiation of 9-fluorenol in evacuated LiY gives a diffuse reflectance spectrum that is very similar to that obtained upon oxygen-purged conditions, except in the 500 nm region. In particular, while the absorption band at 515 nm due to the 9-fluorenyl cation is still clearly visible, the 485 nm shoulder is masked by an additional, longer-lived transient with a maximum around 500 nm. Since this additional species is only observed under vacuum conditions, and is completely quenched in the presence of molecular oxygen, we assign it as the 9-fluorenyl radical produced by photohomolysis of 9-fluorenol within LiY. This assignment is consistent with the known maximum of the 9-fluorenyl radical at 500 nm in solution[31] and also with previous results showing that the 9-fluorenyl radical is produced upon irradiation of 9-fluorenol in methanol.[21,23,26]

Very similar results are observed upon laser excitation of 9-fluorenol within the cavities of dry NaY. Photolysis within this cation-exchanged zeolite also generates the 9-fluorenyl cation, the 9-fluorenyl radical, the metastable triene isomer and the 9-fluorenol radical cation. The triene isomer is again long-lived, and when examined by conventional diffuse reflectance spectroscopy was found to decay very slowly over several minutes with a rate constant of 0.0037 s^{-1}. Interestingly, this rate constant is about 3–4 times slower than that from 9-methyl-9-fluorenol discussed earlier, which is consistent with the accelerating effect of the methyl group in the rearrangement of the intermediate back to the 9-substituted fluorenol derivative.[32]

The 9-fluorenyl cation is even more reactive in NaY where it decays in a first-order manner with a rate constant of 6.6×10^6 s^{-1} and is completely gone by about 800 ns after the laser pulse. In KY, RbY and CsY, photoexcitation of 9-fluorenol resulted in the formation of detectable amounts of triene isomer at 370 nm, radical cation at 370 and 650 nm and 9-fluorenyl radical at 500 nm under vacuum conditions. However, the 9-fluorenyl cation was not detected following the ca. 10 ns laser pulse. The absence of detectable amounts of the carbocation in these zeolites is consistent with our inability to observe the more stable 9-methyl-9-fluorenyl cation with the same series of zeolites, and the expected increase in reactivity of the carbocation as the size of the counterion increases.

As described above, the reactivity of the 9-methyl-9-fluorenyl cation was considerably lower in Naβ than in NaY. As a result, we anticipated that the 9-fluorenyl cation, which is sufficiently long-lived to be observed in NaY, would be readily detectable and even more long-lived in Naβ. Instead, the transient diffuse reflectance spectrum obtained in Naβ is dominated by the intense absorption at 370 nm corresponding to the triene isomer generated by photoinduced rearrangement. Long wavelength absorption with a maximum at 640 nm indicates a small amount radical cation formation is also taking place. In the 500 nm region where the carbocation absorbs, an extremely weak, broad absorption was observed under oxygen conditions. However, the intensity of the absorption in this region was so small that it was difficult to assign the transient, and no kinetic information could be obtained. Under vacuum, the signal intensity increased indicating the formation of the 9-fluorenyl radical.

Effect of added protic reagents

Having established that irradiation of 9-alkyl-9-fluorenol and 9-fluorenol gives the corresponding 9-fluorenyl cations in dry non-protic zeolites, and that these carbocations are sufficiently stabilised within LiY and NaY to be observed, we were curious about the efficiency of the photoheterolysis reaction and the reactivity of the corresponding 9-fluorenyl

cations in the presence of co-adsorbed additives. Of particular relevance with respect to the 9-fluorenol system are protic reagents like water or alcohols. These substances have a considerable influence on the photoheterolysis of 9-fluorenol derivatives in solution and tend to increase the efficiency of the photoreaction compared to non-protic solvents like acetonitrile.[24–26] In addition, such reagents have a wide range of nucleophilicity depending on the structure of the alcohol, and thus can be used to modulate the lifetime of the carbocation.

When 9-methyl-9-fluorenol or 9-fluorenol is photolysed in LiY or NaY containing co-adsorbed water (3–6% by weight), the transient absorption band due to the corresponding carbocation observed under dry conditions is no longer visible. The kinetic traces monitored at 485 or 515 nm indicate that the 9-fluorenyl cations are not present at any time following the laser pulse. One explanation for our inability to observe the carbocations in hydrated zeolites is that photoheterolysis is no longer occurring under these conditions. However, this explanation is contrary to a large body of experimental evidence in solution indicating that photoheterolysis efficiency is enhanced by water.[23–26] An alternative explanation is that the carbocations are still generated in the zeolite cavities, but are then rapidly quenched within the duration of the laser pulse by the co-adsorbed water. Complete quenching of the carbocation is consistent with the nucleophilic behaviour of water towards reactive carbocations. In fact, on the basis of the short lifetime of 275 ps for the 9-methyl-9-fluorenyl cation and $<$20 ps for the 9-fluorenyl cation in 9:1 water/methanol solutions[23] and previous observations that even less reactive carbocations like the 4-methoxycumyl cation are completely quenched in hydrated zeolites,[18] it would have been remarkable for the 9-fluorenyl cations to have survived sufficiently long to be observed upon hydration of the zeolite.

Results obtained upon laser photolysis of 9-methyl-9-fluorenol within hydrated Naβ (3% by weight) provide evidence that photoheterolysis is actually enhanced in the presence of co-adsorbed water. Under these conditions, the carbocation is shorter-lived (k_{hyd}=3×10^6 s^{-1}) relative to dry conditions due to nucleophilic quenching by water, but still has a sufficiently long lifetime to be readily detected using the nanosecond system. As a result, we were able to measure the intensity of the absorption of the carbocation immediately after the laser pulse and thus determine that the inclusion of small amounts of co-adsorbed water significantly enhances the yield of the 9-methyl-9-fluorenyl carbocation at 485 nm by a factor of two compared to that under dry conditions. The results also showed that the relative yield of the metastable triene isomer at 370 nm dropped considerably in the presence of water. Thus, it is apparent that the co-adsorbed water accelerates heterolysis from the excited state, and increases the efficiency of carbocation formation at the expense of the other photochemical reactions such as rearrangement to the triene isomer.

In order to obtain stronger evidence that the photoheterolysis reaction within alkali metal Y-zeolites can be enhanced by protic reagents, an alcohol with reduced nucleophilicity was employed instead of water. It has been previously observed that photoheterolysis is the dominant reaction of photoexcited 9-fluorenols in HFIP and that in this solvent the 9-fluorenyl cation is sufficiently long-lived to be easily observed on the nanosecond timescale.[22] Thus, HFIP should be an ideal additive with which to examine the influence of protic reagents on the intrazeolite yield of the photoheterolysis reaction.

As shown in Fig. 3 (top), the amount of co-adsorbed HFIP did indeed have a dramatic effect on the efficiency of the photoheterolysis reaction, with the yield of the 9-methyl-9-fluorenyl cation doubling upon going from a dry zeolite sample with no HFIP to a sample containing 10% HFIP by weight. Rate constants for the decay of the carbocations were also affected, but unlike the situation when water was added where the rate constants became larger, HFIP actually causes the rate constants to decline, Fig. 3 (bottom).

The influence of co-adsorbed HFIP on the generation and reactivity of the 9-methyl-9-fluorenyl cation in Naβ was also investigated. In this case, the already slow rate constant for carbocation decay in Naβ changed little as a function of HFIP content. However, the yield of the 9-methyl-9-fluorenyl cation again increased with increasing amounts of added HFIP, with the efficiency doubling in the presence of 10% HFIP by weight.

The influence of 1,1,1,3,3,3-hexafluoro-2-propanol-*d* (HFIP-OD) on the absolute yields of the 9-methyl-9-fluorenyl cation in NaY and Naβ was also measured relative to the undeuterated analog. The results demonstrate that HFIP-OD is significantly less effective than HFIP-OH in promoting photoheterolysis of 9-methyl-9-fluorenol within

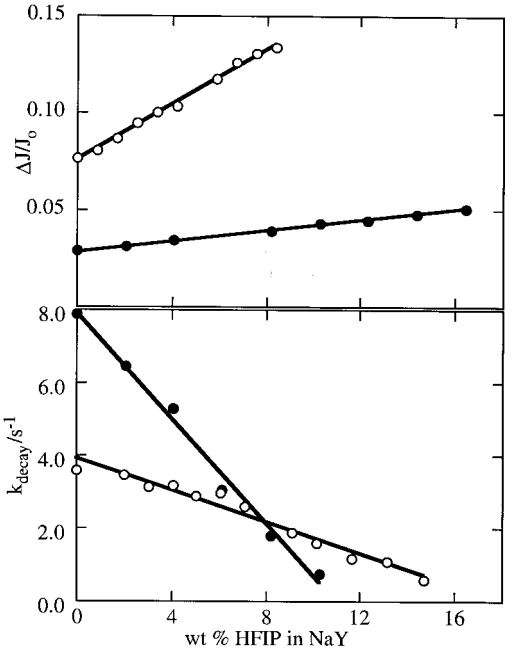

Figure 3. (Top) Maximum diffuse reflectance due to the formation of the (●) 9-fluorenyl cation at 515 nm and (○) 9-methyl-9-fluorenyl cation at 485 nm in NaY containing different amounts of HFIP. (Bottom) First-order rate constants for the decay of the (●) 9-fluorenyl cation and the (○) 9-methyl-9-fluorenyl cation generated in NaY containing different amounts of HFIP.

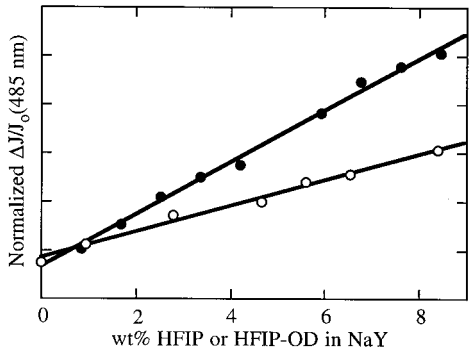

Figure 4. Maximum diffuse reflectance due to the formation of the 9-methyl-9-fluorenyl cation at 485 nm at different amounts of (●) HFIP and (○) HFIP-OD in NaY.

both NaY and Naβ. In NaY, Fig. 4, the change in initial reflectance density of the 9-methyl-9-fluorenyl cation as a function of HFIP-OH is twice that produced by including the same amount of HFIP-OD into the sample. In Naβ, a similar result is observed, with the non-deuterated HFIP-OH being 1.6-fold more effective in enhancing carbocation formation compared to the deuterated HFIP-OD.

Discussion

Reactivity of 9-fluorenyl cations in non-protic zeolites

Evidence that illustrates the low thermodynamic stability of the 9-fluorenyl cation includes the lack of success in generating and observing the carbocation under strong or superacid conditions,[33] and the unusually low pK_R value of −17.3 for 9-fluorenol[34] compared to the pK_R of −13.3 for the diphenylmethanol.[35] The kinetic instability of the fluorenyl cation has also been well documented. For example, in wholly aqueous solution, the rate constant for the decay of the carbocation is about 10^{11} s^{-1} which is considerably faster than the rate constant for the diphenylmethyl cation under the same conditions.[23]

The 9-fluorenyl cation has been observed previously in solution using nanosecond laser photolysis, but only under a unique set of conditions where the carbocation is strongly kinetically stabilised by the weakly-nucleophilic and highly polar solvent HFIP.[22] The present work therefore describes only the second set of experimental conditions encountered whereby the 9-fluorenyl cation is sufficiently long-lived to be observed on the nanosecond time-scale. These results therefore give clear evidence that zeolite cavities provide a weakly-nucleophilic, polar environment that is exceptional in its ability to enhance the lifetime of otherwise extremely reactive positively charged species.

The fact that the 9-fluorenyl cation could be detected in LiY and NaY is even more remarkable upon recognition that these are non-proton containing zeolites. Thus, the enhanced lifetime of the carbocation in these zeolites is not due a thermodynamic effect whereby the highly acidic environment shifts an otherwise unfavourable equilibrium to the side of the carbocation, nor is it due to a situation in which the strength of the nucleophilic sites in the zeolite is reduced by protonation.

Even though we were able to observe the 9-fluorenyl cation in LiY and NaY, the carbocation is still very reactive compared to other similar species. This is evident upon comparing the rate constant for the decay of the 9-fluorenyl cation to rate constants for the decay of other carbocations under the same conditions, Table 1. For example, we have previously found that the stabilised 4-methoxycumyl cation decays with a rate constant of 4×10^4 s^{-1} in LiY that is 75-fold slower than the decay of the 9-fluorenyl cation in the same zeolite.[18] In addition, the diphenylmethyl cation decays with a rate constant of 5.5×10^5 s^{-1} in LiY[20] that is five-fold slower than that of the 9-fluorenyl cation. This order in reactivity is the same as that observed in solution. Thus, while the Y zeolites are suitable hosts to increase the lifetime of highly reactive carbocations like the 9-fluorenyl cation to the point where they can be observed on the nanosecond time-scale, the zeolites do not change the reactivity order from that observed in solution. On the other hand, the 75-fold difference between the reactivity of the 9-fluorenyl cation and that for the 4-methoxycumyl cation in LiY is remarkably smaller than the 10^4-fold difference in reactivity between the same carbocations in 2,2,2-trifluoroethanol (TFE).[36] Thus, the environment within the zeolite cavities provides a dramatic levelling effect whereby the relative reactivity of carbocations is less sensitive to relative thermodynamic stability than that observed in solution.

As shown in Fig. 3 (bottom), the lifetimes of the fluorenyl cations within NaY could be strongly enhanced by adding relatively small amounts of the slightly acidic, weakly nucleophilic alcohol HFIP. Since the zeolite samples were carefully prepared to exclude the presence of unwanted nucleophiles such as water, the decay of the carbocation presumably involves addition of the weakly nucleophilic oxygen in a Si–O–Al bridge (Scheme 2a) to generate a framework bound alkoxy species.[12,18] A reasonable explanation for the effect of the HFIP is that it interferes with this nucleophilic addition reaction by forming a hydrogen bond with the reactive framework oxygen as shown in Scheme 2b. Alternatively, the weakly nucleophilic oxygen of HFIP may interact with the cationic centre of the

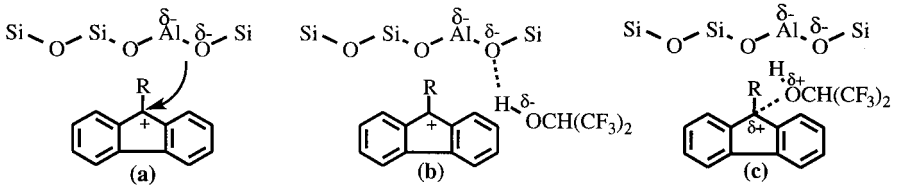

Scheme 2.

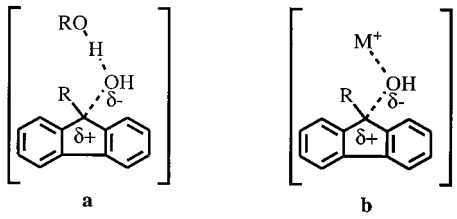

Scheme 3.

9-fluorenyl cation, thus inhibiting an interaction between the carbocation and the nucleophilic framework oxygen, Scheme 2c.

Mechanism of carbocation formation

Several studies have demonstrated that carbocation formation in solution takes place by simple photoheterolysis of the C–O bond. Wan has argued that this process is not acid catalysed,[24,26] but the fact that protic solvents are needed for carbocation formation to be efficient suggests that protons from the solvent may participate in the product determining step by interacting with the oxygen of the leaving hydroxide ion, Scheme 3a. In the dry zeolite, no protic reagent is available, so stabilisation of the hydroxide ion by a hydrogen-bonding interaction is not possible. However, the zeolite cavities are occupied by Li^+ or Na^+ that possess sufficiently high Lewis acidity to play the role otherwise taken by the proton and help stabilise the hydroxide ion as the C–O bond in the excited state cleaves, Scheme 3b.

The photoheterolysis reaction of fluorenols in solution is also strongly dependent on the ionising power of the solvent.[24,26] The fact that fluorenyl cation formation occurs in LiY and NaY demonstrates clearly that the environments of these zeolites are sufficiently ionising to support charge-separation reactions. This is consistent with recent results showing that the ionising ability of LiY and NaY zeolites is similar to that of neat HFIP.[37]

The observation that carbocation generation via photoheterolysis is enhanced within alkali metal zeolites containing co-adsorbed water or HFIP is consistent with the protic additive actively participating in the C–OH bond cleavage of the excited state fluorenols. Thus, in a manner similar to that represented in Scheme 3a, the water or HFIP incorporated within the zeolite cavity can interact with the oxygen of the excited fluorenol and stabilise the incipient negative charge on the developing hydroxide ion. Alternatively, inclusion of water or HFIP may simply enhance the internal ionising ability of the zeolite microenvironment. In this case, the additive simply plays a passive role by making the zeolite cavity more hospitable for carbocation formation. The isotope effect studies were carried out in an attempt to distinguish between the two possible roles played by the added alcohol. The results clearly show that the efficiency of carbocation formation decreases significantly in the presence of the deuterated HFIP. This behaviour is expected for the mechanism in which the alcohol shares its proton with the oxygen of the leaving group as the product determining step progresses, and thus provides evidence for the direct participation of the added alcohol.

In conclusion, our results clearly show that alkali metal cation-exchanged zeolites have sufficient polarity and are suitably non-nucleophilic to enhance the lifetimes of reactive carbocations like 9-alkyl-9-fluorenyl cations and even the extremely reactive 9-fluorenyl cation to the point where they can be observed using nanosecond laser techniques. In addition, the generation and reactivity of these species can be modulated by changing the alkali metal cation and by the addition of hydroxyl group containing additives. When the additive is nucleophilic like water, the reactivity is increased to the point where the carbocation is no longer observed. Conversely, HFIP actually decreases the reactivity of the carbocation, presumably by inhibiting the reaction of the carbocation with nucleophilic sites in the framework.

Experimental

Materials

9-Fluorenol is commercially available (Aldrich) and was used as received. 9-Methyl-, 9-ethyl- and 9-isopropyl-9-fluorenol were prepared form 9-fluorenone and the appropriate Grignard reagent and purified by recrystallization from ethanol. 1,1,1,3,3,3-Hexafluoro-2-propanol (HFIP) and 1,1,1,3,3,3-hexafluoro-2-propanol-*d*(HFIP-OD) are commercially available from Aldrich. NaY(Si/Al=2.4) was obtained from Aldrich while Naβ (Si/Al=18) was purchased from the P.Q. Corporation. All zeolites were used as received after activation at 400°C for 16 h to remove any co-incorporated water. The exchanged zeolites were prepared by stirring NaY with 1 M aqueous solutions of the corresponding chlorides (LiCl, KCl, RbCl, CsCl) at 80°C for 1 h. The zeolites were then washed until no chlorides appeared in the washing water and dried under vacuum. This procedure was repeated three times and the zeolite was calcinated between washings. The percent exchange is 47% for LiY, 97% for KY, 44% for RbY and 47% for CsY.

Sample preparation

The 9-fluorenols were incorporated into NaY using hexanes as a carrier solvent. Samples for laser experiments were prepared such that the loading level was approximately one molecule in every 10 supercages. The typical procedure involved introducing ca. 1 mL of a stock solution of the organic compound to ca. 250 mg of activated zeolite in 20 mL of hexane. The hexane slurry was stirred for ca. 1 h, after which the suspension was centrifuged and the isolated zeolite washed using hexane and dried under vacuum, 10^{-3} Torr. UV analysis of the combined decants indicated that 100% of the organic precursor was incorporated within NaY. During the incorporation of the precursor into the zeolite framework the utmost care was taken to ensure that the zeolite was never exposed to moisture from the air or any other source. After vacuum drying for several hours, the zeolite samples were transferred to laser cells in a nitrogen filled glove bag, and then re-evacuated to 10^{-3} Torr for an additional 10–12 h before the photolysis experiments. The procedure for incorporation of the

9-fluorenols into the other cation-exchanged zeolites was essentially identical to that for incorporation into NaY. The initial amount of 9-fluorenol was adjusted to account for the reduced percent incorporation in the larger alkali cation zeolites, such that the final concentration was one molecule in every 10 supercages for all faujasites studied.

Hydration experiments

Zeolite samples were hydrated by exposing a known quantity of the vacuum-dried 9-fluorenol/zeolite composites to the atmosphere. The sample was spread into a thin layer on a shallow dish to allow for efficient hydration. The changes in sample mass due to water uptake were monitored until no further change was observed. Typical values of water uptake were 3–6% by weight.

HFIP experiments

Zeolite samples used in the HFIP experiments were prepared by vapour phase adsorption of the HFIP in dry zeolite/9-fluorenol composites. This typically involved introducing the liquid alcohol in μL increments with a syringe through the top of a sealed laser cell containing a small quantity (ca. 100–200 mg) of the composite. The laser cell was then heated slightly with a low temperature heat gun to vaporise the alcohol and the material was shaken to thoroughly mix the contents. The sample was allowed to cool to room temperature before conducting the laser experiments.

Time-resolved diffuse reflectance

Time-resolved diffuse reflectance experiments were carried out using a nanosecond laser system. The excitation source was a Lambda–Physik excimer laser (308 nm, 100 mJ, 10 ns/pulse). The transient signals from the monochromator-PMT detection system were captured using a Tektronix 620 digitizer and then transferred via a GPIB interface to a Power Macintosh 7100 computer which controls the laser system using a program written with LabView 3.0 software. The experimental setup for time resolved diffuse reflectance is similar to that described in detail previously.[17] The samples were contained in quartz cells constructed with 3×7 mm^2 tubing and were either evacuated under reduced pressure (10^{-3} Torr) and sealed or purged with oxygen for a minimum of 20 min prior to photolysis. The data analysis was based on the fraction of reflected light absorbed by the transient (reflectance change $\Delta J/J_o$) where J_o is the reflectance intensity before excitation and ΔJ is the change in the reflectance after excitation. Observed rate constants for the decay of the 9-fluorenyl cations were calculated by non-linear least squares fitting of the decay curves at a selected wavelength to a first-order expression.

Conventional diffuse reflectance

Conventional diffuse reflectance spectra and kinetics were obtained using a Cary 100 Bio UV–Visible spectrophotometer with a Labsphere adapter for diffuse reflectance experiments. 9-Methyl-9-fluorenol or 9-fluorenol/zeolite composites were prepared in the same manner as for the fast time-resolved laser experiments, and then placed in a standard sample cell with a quartz window. The composites were then subjected to 10–20 308-nm laser pulses, and within 30 s placed into the sample holder of the spectrophotometer. Changes in diffuse reflectance at 370 nm were measured as a function of time to obtain rate constants for the decay of the metastable triene isomer. No other absorption bands were observed in these long-time scale experiments.

Acknowledgements

We gratefully acknowledge the Natural Science and Engineering Research Council of Canada (NSERC) and Dalhousie University for financial support of this research. M. A. O. is the recipient of an NSERC graduate scholarship and F. L. C. is the recipient of an NSERC-WFA.

References

1. Corma, A. *Chem. Rev.* **1995**, *95*, 559–614.
2. Cano, M. L.; Fornes, V.; Garcia, H.; Miranda, M. A.; Perez-Prieto, J. *J. Chem. Soc., Chem. Commun.* **1995**, 2477–2478.
3. Cano, M. L.; Cozens, F. L.; Fornes, V.; Garcia, H.; Scaiano, J. C. *J. Phys. Chem.* **1996**, *100*, 18145–18151.
4. Cano, M. L.; Corma, A.; Fornes, V.; Garcia, H.; Miranda, M. A.; Baerlocher, C.; Lengauer, C. *J. Am. Chem. Soc.* **1996**, *118*, 11006–11013.
5. Cozens, F. L.; Garcia, H.; Scaiano, J. C. *Langmuir* **1994**, *10*, 2246–2249.
6. Cozens, F. L.; Bogdanov, R.; Regimbald, M.; Garcia, H.; Marti, V.; Scaiano, J. C. *J. Phys. Chem. B.* **1997**, *101*, 6821–6829.
7. Liu, X. L.; Iu, K.; Thomas, J. K.; He, H.; Klinowski, J. *J. Am. Chem. Soc.* **1994**, *116*, 11811–11818.
8. Kiricsi, I.; Forster, H.; Tasi, G.; Nagy, J. B. *Chem. Rev.* **1999**, *99*, 2085–2114.
9. Tao, T.; Maciel, G. E. *J. Am. Chem. Soc.* **1995**, *117*, 12889–12890.
10. Xu, T.; Haw, J. F. *J. Am. Chem. Soc.* **1994**, *116*, 10188–10195.
11. Xu, T.; Haw, J. F. *J. Am. Chem. Soc.* **1994**, *116*, 7753–7759.
12. Haw, J. F.; Nicholas, J. B.; Xu, T.; Beck, L. W.; Ferguson, D. B. *Acc. Chem. Res.* **1996**, *29*, 259–267.
13. Xu, T.; Barich, D. H.; Goguen, P. W.; Song, W.; Wang, Z.; Nicholas, J. B.; Haw, J. F. *J. Am. Chem. Soc.* **1998**, *120*, 4025–4026.
14. Nicholas, J. B.; Haw, J. F. *J. Am. Chem. Soc.* **1998**, *120*, 11804–11805.
15. Kazansky, V. B. *Acc. Chem. Res.* **1991**, *24*, 379–383.
16. Cano, M. L.; Corma, A.; Fornes, V.; Garcia, H. *J. Phys. Chem.* **1995**, *99*, 4241–4246.
17. Cozens, F. L.; Cano, M. L.; Garcia, H.; Schepp, N. P. *J. Am. Chem. Soc.* **1998**, *120*, 5667–5673.
18. Cozens, F. L.; O'Neill, M. A.; Schepp, N. P. *J. Am. Chem. Soc.* **2000**, *122*, 6017–6027.
19. Cozens, F. L.; O'Neill, M.; Schepp, N. P. *J. Am. Chem. Soc.* **1997**, *119*, 7583–7584.
20. Cozens, F. L.; Ortiz, W.; O'Neill, M.; Shea, S.; Schepp, N. P. Unpublished results.
21. Gaillard, E.; Fox, M. A. P.; Wan, P. *J. Am. Chem. Soc.* **1989**, *111*, 2180–2186.
22. McClelland, R. A.; Mathivanan, N.; Steenken, S. *J. Am. Chem. Soc.* **1990**, *112*, 4857–4861.

23. Mecklenburg, S. L.; Hilinski, E. F. *J. Am. Chem. Soc.* **1989**, *111*, 5471–5472.
24. Wan, P.; Krogh, E. *J. Chem. Soc., Chem. Commun.* **1985**, 1207–1208.
25. Krogh, E.; Wan, P. *Tetrahedron Lett.* **1986**, *27*, 823–826.
26. Wan, P.; Krogh, E. *J. Am. Chem. Soc.* **1989**, *111*, 4887–4895.
27. Delcourt, M. O.; Rossi, M. J. *J. Phys. Chem.* **1982**, *86*, 3233–3239.
28. Falvey, D. E.; Schuster, G. B. *J. Am. Chem. Soc.* **1986**, *180*, 7419–7420.
29. Jaeger, D. A. *J. Am. Chem. Soc.* **1974**, *96*, 6216–6217.
30. Cozens, F. L.; Pincock, A.; Pincock, J. A.; Smith, R. *J. Org. Chem.* **1998**, *636*, 434–435.
31. Wong, P. C.; Griller, D.; Scaiano, J. C. *J. Am. Chem. Soc.* **1981**, *103*, 5934–5935.
32. This 3–4 fold difference in reactivity is identical to that observed for the rearrangement of the triene isomers of 9-methyl-9-fluorenol and 9-fluorenol in methanol.
33. Olah, G. A.; Surya Prakash, G. K.; Liang, G.; Westerman, P. W.; Kunde, K.; Chandrasekhar, J.; v. R. Schleyer, P. *J. Am. Chem. Soc.* **1980**, *102*, 4485–4492.
34. Wayner, D. D. M.; McPhee, D. J.; Griller, D. *J. Am. Chem. Soc.* **1988**, *110*, 132–137.
35. Deno, N. C.; Jaruzelski, J. J.; Schriesheim, A. *J. Am. Chem. Soc.* **1955**, *77*, 3044–3051.
36. Cozens, F. L. PhD Thesis, University of Toronto, 1992.
37. Ortiz, W.; Cozens, F. L.; Schepp, N. P. *Org. Lett.* **1999**, *1*, 531–534.